



**HAL**  
open science

# Solvent-Free Epoxidation of Olefins Catalyzed by “[MoO<sub>2</sub> (SAP)]”: A New Mode of tert -Butylhydroperoxide Activation

Julien Morlot, Nicolas Uyttebroeck, Dominique Agustin, Rinaldo Poli

## ► To cite this version:

Julien Morlot, Nicolas Uyttebroeck, Dominique Agustin, Rinaldo Poli. Solvent-Free Epoxidation of Olefins Catalyzed by “[MoO<sub>2</sub> (SAP)]”: A New Mode of tert -Butylhydroperoxide Activation. ChemCatChem, 2013, 5 (2), pp.601-611. 10.1002/cctc.201200068 . hal-02908276

**HAL Id: hal-02908276**

**<https://hal.science/hal-02908276>**

Submitted on 29 Jul 2021

**HAL** is a multi-disciplinary open access archive for the deposit and dissemination of scientific research documents, whether they are published or not. The documents may come from teaching and research institutions in France or abroad, or from public or private research centers.

L'archive ouverte pluridisciplinaire **HAL**, est destinée au dépôt et à la diffusion de documents scientifiques de niveau recherche, publiés ou non, émanant des établissements d'enseignement et de recherche français ou étrangers, des laboratoires publics ou privés.

# Solvent-free epoxidation of olefins catalyzed by “[MoO<sub>2</sub>(SAP)]”: a new mode of TBHP activation

Julien Morlot,<sup>[a,b]</sup> Nicolas Uyttebroeck,<sup>[a,b]</sup> Dominique Agustin,<sup>\*[a,b]</sup> Rinaldo Poli<sup>\*[a,c]</sup>

The mononuclear molybdenum complexes [MoO<sub>2</sub>(acac)<sub>2</sub>] (**1**), [MoO<sub>2</sub>(SAP)(MeOH)] (**2**), and dinuclear oxomolybdic complexes [MoO<sub>2</sub>L]<sub>2</sub> (L = SAP (**5**), SAE (**6**), SAMP (**7**)) have been investigated as (pre)catalysts for the epoxidation of olefins under solvent-free conditions, using tert-butylhydroperoxide (TBHP, 70% in water) as oxidant. Complexes **6** and **7**, although active, are limited by ligand hydrolysis during the catalytic process, whereas complexes **2** and **5** are not altered under catalytic conditions and yield essentially the

same selectivity and activity, which is not suppressed by excess MeOH. Although these catalysts are less active than **1**, their selectivity is higher (97-98%). DFT calculations are consistent with the active form of the catalyst being the 5-coordinate [MoO<sub>2</sub>(SAP)]. The oxidant is activated by forming a weak adduct stabilized by a very loose Mo...O interaction and a hydrogen bond, predisposing it to the oxygen transfer to external olefin by a mechanism closely related to Bartlett's epoxidation with peroxyacids.

## Introduction

Epoxides are powerful building blocks in synthetic chemistry, since nucleophilic ring-opening leads to a large variety of functional products from small-size molecules (aminoalcohols, diols, etc...)<sup>[1-2]</sup> to oligomer and polymers.<sup>[3-5]</sup> In general, epoxides are efficiently obtained by oxygen atom transfer to olefins, either using stoichiometric organic peracids such as *m*-chloroperbenzoic acid (*m*CPBA)<sup>[6]</sup> or MeCOOOH,<sup>[7-8]</sup> or milder oxygen transfer agents in metal-catalyzed processes. In the latter case, the terminal oxidant may be PhIO, NaClO,<sup>[9]</sup> *tert*-butylhydroperoxide (TBHP) in decane or in water,<sup>[10]</sup> H<sub>2</sub>O<sub>2</sub> in water<sup>[11]</sup> or in an organic solvent,<sup>[12]</sup> H<sub>2</sub>O<sub>2</sub>-urea in an ionic liquid,<sup>[13]</sup> or even O<sub>2</sub>.<sup>[14-15]</sup> Most of these reactions are performed in organic solvents (acetonitrile,<sup>[12]</sup> dichloroethane,<sup>[16]</sup> aromatics<sup>[17-18]</sup> or alcohols<sup>[19]</sup>). With the increasing demand for cleaner and environmentally friendlier processes,<sup>[20]</sup> there is great current interest in moving away from the rather common use of chlorinated or aromatic solvents<sup>[21]</sup> and to use green oxidants. At a first glance, TBHP appears as less ideal than H<sub>2</sub>O<sub>2</sub> or O<sub>2</sub>, but the low reagent and process costs coupled with the added value of the by-product *t*BuOH as an octane booster in gasoline<sup>[22]</sup> continues to justify interest in this reagent. On one hand, organic solvents are expected to increase the reaction rate by confining all components in a single phase. On the other hand, organic solvents can be hazardous and their recycling has a cost. In our research, we focus on the catalytic application of transition metal oxo-complexes in the (ep)oxidation of unsaturated substrates under experimental conditions fulfilling the principles of green chemistry.<sup>[23-24]</sup>

Among the catalytic metals, molybdenum is the most commonly employed one in industrial processes<sup>[25-26]</sup> and is also used in Nature by molybdoenzymes.<sup>[27-28]</sup> Generally used (pre)catalysts have general formula [MoO<sub>2</sub>X<sub>2</sub>L<sub>2</sub>] (X = Cl, Br and L<sub>2</sub> = bidentate ligand<sup>[29-31]</sup> or X<sub>2</sub>L<sub>2</sub> = tetradentate dianionic ligand).<sup>[32]</sup> The commercially available and easily accessible [MoO<sub>2</sub>(acac)<sub>2</sub>] (**1**) was described as one of the best molecular (pre)catalysts for the homogeneous catalytic (ep)oxidations of olefins with

TBHP/decane in organic solvents<sup>[10, 19, 33-35]</sup>. Unfortunately, because of poor solubility in water and hydrolytic instability,<sup>[36-37]</sup> this complex is unsuitable for aqueous/organic biphasic systems. For instance, **1** catalyzes cyclohexene epoxidation to cyclohexanediol by aqueous TBHP,<sup>[10]</sup> but could not be recovered and reused under these experimental conditions. Stable alternatives to **1** are therefore of interest. Neutral dioxomolybdic complexes with ONO tridentate Schiff base ligands (L) seem good candidates.<sup>[21, 32, 38-43]</sup> These complexes may exist in a dinuclear, oxo-bridged form [MoO<sub>2</sub>L]<sub>2</sub> or as mononuclear octahedral adducts with a donor molecule D, [MoO<sub>2</sub>L(D)]. Several of these have been used as oxygen transfer agents or sulfoxidation catalysts,<sup>[21, 44-50]</sup> and also for epoxidation reactions in organic solvents, but only in the [MoO<sub>2</sub>L(D)] form.<sup>[21, 32, 41, 51-54]</sup> Recently, the immobilization of monomeric complexes for application in heterogenized homogeneous catalysis conditions has been justified since “*μ-oxo dimeric complexes lead to irreversible catalyst deactivation*”.<sup>[55-56]</sup> To our knowledge, the catalytic epoxidation properties of [MoO<sub>2</sub>L]<sub>2</sub> complexes under homogeneous conditions – i.e. not grafted to polymers or inorganic surfaces - under “green” conditions have not been reported and this has inspired our work in this area.

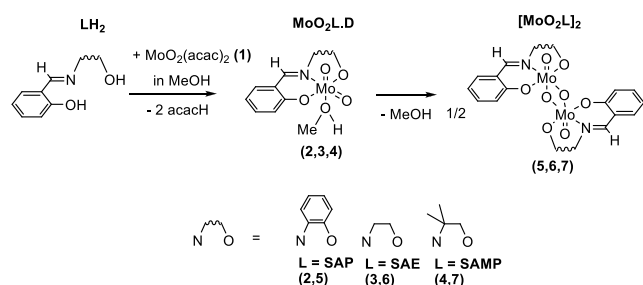
An additional interest in these systems is mechanistic. Contrary to most other MoO<sub>2</sub>-based catalytic systems, which feature a (pseudo)octahedral coordination environment, where the oxidant TBHP may only add by proton transfer to an oxido

- [a] Mr. J. Morlot, Mr. N. Uyttebroeck, Dr. D. Agustin, Prof. R. Poli  
CNRS; LCC (Laboratoire de Chimie de Coordination); Université de  
Toulouse; UPS, INPT  
205, route de Narbonne, F-31077 Toulouse, France  
Fax: +33-561553003  
E-mail: [dominique.agustin@iut-tlse3.fr](mailto:dominique.agustin@iut-tlse3.fr)  
[rinaldo.poli@cc-toulouse.fr](mailto:rinaldo.poli@cc-toulouse.fr)
- [b] Université de Toulouse; Institut Universitaire de Technologie Paul  
Sabatier  
Département de Chimie  
Av. Georges Pompidou, BP 20258, F-81104 Castres Cedex, France
- [c] Institut Universitaire de France  
103, bd Saint-Michel, 75005 Paris, France

Supporting information for this article is available on the WWW  
under <http://dx.doi.org/10.1002/cctc.200xxxxx>.

ligand generating (pseudo)seven-coordinate Mo(OH)(OO*t*Bu) intermediates, these ONO systems, via release of the loosely bonded MeOH, produce a 5-coordinate, potentially more active [MoO<sub>2</sub>L] catalyst to which TBHP may also coordinate as a neutral ligand.

We have recently revisited the synthetic and coordination aspects of dioxomolybdenum complexes with the tridentate ONO ligands salicylideneaminophenol (H<sub>2</sub>SAP), salicylideneaminoethanol (H<sub>2</sub>SAE) and salicylideneaminomethylpropanol (H<sub>2</sub>SAMP), Scheme 1.<sup>[38-39]</sup> These ligands and the associated complexes are inexpensive and accessible by simple preparative procedures. We now describe the epoxidation activity of [MoO<sub>2</sub>L]<sub>2</sub> complexes (L= SAP (5), SAE (6), SAMP (7)) and [MoO<sub>2</sub>(SAP)(MeOH)] (2) towards *cis*-cyclooctene using TBHP in water as oxidant without any added solvent. The results have been compared to the catalytic activity of 1 under the same experimental conditions. Mechanistic aspects of the process are also investigated with the help of DFT calculations.



Scheme 1. Synthetic procedures for [MoO<sub>2</sub>L(MeOH)] and [MoO<sub>2</sub>L]<sub>2</sub> compounds.

## Results and Discussion

### 1. Ligands and complexes: synthesis and characterization.

The LH<sub>2</sub> ligands (L = SAP, SAE, SAMP)<sup>[57-58]</sup> were synthesized from 2-hydroxybenzaldehyde and aminophenol, aminoethanol and aminomethylpropanol, respectively, by a new procedure in water (see Experimental section). Their reaction with 1 to yield the known mononuclear<sup>[49, 59-60]</sup> 2-4 and dinuclear<sup>[61-62]</sup> 5-7 has also been improved as described in the Experimental section. New IR and TGA investigations are reported here.

The major problem of the [MoO<sub>2</sub>L(D)] complex is weak binding of the D ligand. When this is a volatile compound such as MeOH, the compound may partially transform into the dinuclear [MoO<sub>2</sub>L]<sub>2</sub>. The [MoO<sub>2</sub>L(D)] and [MoO<sub>2</sub>L]<sub>2</sub> structures show distinct features in the IR spectrum, which can thus be used to evaluate the ratio between the two forms. The full spectra are reported in SI (Figure S1) and relevant bands for the Mo=O and Mo-O-Mo stretchings are listed in Table 1. The assignment of these bands is backed up by DFT calculations on compounds 2, 5 and 6. Two broad bands attributed to Mo=O vibrations are observed around 930 cm<sup>-1</sup> for 2-4, whereas only one strong and broad band around 920 cm<sup>-1</sup> is visible for 5-7, plus a complex pattern around 820-840 cm<sup>-1</sup> due to the Mo<sub>2</sub>(μ-O)<sub>2</sub> moiety. The calculated frequencies are ca. 80 cm<sup>-1</sup> higher than the experimental ones, but the pattern is in good agreement with the observed spectra (see SI, Figure S2). According to the calculations, the terminal Mo=O bonds in 5 and 6 do not experience strong vibrational coupling, yielding nearly

degenerate normal modes and justifying the observation of a single band.

2	3	4	5	6	7	Assignment <sup>[b]</sup>
			816 909(947)	839 884(813) 899(210)	841	(Mo-O-Mo) <sub>as</sub> + (Mo=O) <sub>as</sub>
914 977(230)	902	911	928 1001(300)	912 996(293) 1000(70)	928	(Mo=O) <sub>as</sub> (+ (Mo-O-Mo) <sub>as</sub> for 5 and 6)
933 999(164)	926	929				(Mo=O) <sub>s</sub>

[a] For compounds 2, 5 and 6, the values in italics correspond to those obtained from the DFT study, with values in parentheses corresponding to the intensities in KM/mole. [b] Based on the DFT calculations. All modes also contained a small contribution of the out-of-plane C-H bending vibration.

The thermograms of the SAP pair of complexes (2 and 5) are shown in Figure 1, the others being available in the SI (Figure S3). All relative mass loss data are listed in Table 2. All [MoO<sub>2</sub>L(MeOH)] complexes release MeOH below 150°C, leading to “MoO<sub>2</sub>L” species. A second mass loss occurs at much higher temperature, corresponding to the release of L (presumably as H<sub>2</sub>L) compensated by the addition of O, to yield MoO<sub>3</sub>.<sup>[39]</sup> The TGA of the dinuclear compounds 5-7 exhibit only the second process, with similar shape to that of the corresponding mononuclear complex, indicating that the thermolytic decomposition of the methanol adducts 2-4 occurs with 5-7 as intermediates. Although the TGA of freshly prepared 2-4 gave the correct mass loss values,<sup>[50, 63]</sup> storage in air led to slow methanol dissociation in favor of the dinuclear form,<sup>[63]</sup> as verified by both IR and TGA. Hence, complexes [MoO<sub>2</sub>L]<sub>2</sub> appear as better “ready to use” (pre)catalysts, because they are relatively stable under the same storage conditions.

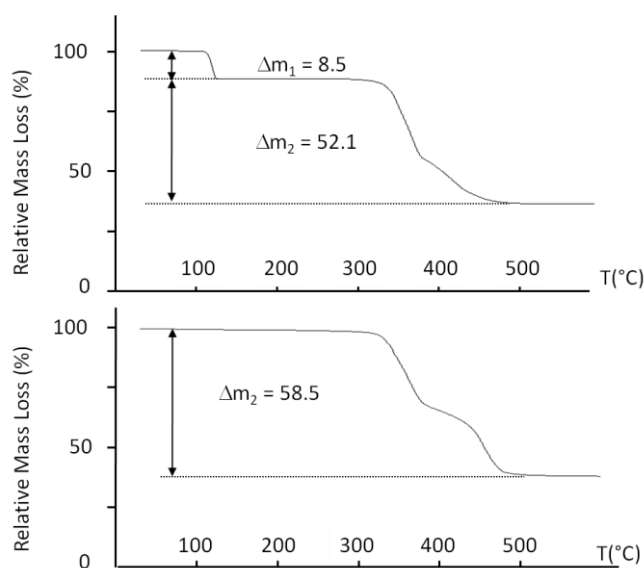


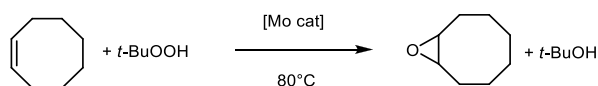
Figure 1. Thermograms of compounds 2 (above) and 5 (below).

Table 2. Experimental (theoretical) relative mass losses from the TGA of  $[\text{MoO}_2\text{L}(\text{MeOH})]$  and  $[\text{MoO}_2\text{L}_2]$  complexes

Compound		$\Delta m_1(50-150^\circ\text{C})/\%$	$\Delta m_2(250-600^\circ\text{C})/\%$
		Exp (theo)	Exp (theo)
$[\text{MoO}_2(\text{SAP})(\text{MeOH})]$	<b>2</b>	8.5 (8.6)	52.1 (52.6)
$[\text{MoO}_2(\text{SAE})(\text{MeOH})]$	<b>3</b>	9.6 (9.9)	46.1 (45.6)
$[\text{MoO}_2(\text{SAMP})(\text{MeOH})]$	<b>4</b>	9.1 (9.1)	50.4 (49.9)
$[\text{MoO}_2(\text{SAP})_2]$	<b>5</b>	-	58.5 (57.6)
$[\text{MoO}_2(\text{SAE})_2]$	<b>6</b>	-	51.1 (50.5)
$[\text{MoO}_2(\text{SAMP})_2]$	<b>7</b>	-	51.1 (54.9)

## 2. Catalytic investigations

As mentioned above, "MoO<sub>2</sub>L" complexes with ONO tridentate Schiff base ligands have only been previously used in catalyzed olefin epoxidation as alcohol adducts in organic solvents.<sup>[32, 52-54]</sup> Cyclooctene epoxidation by aqueous TBHP (Scheme 2) was investigated in the absence of organic solvent, according to our established protocol,<sup>[64-66]</sup> in the presence of complexes **5-7** and compared with the performance of **1** under the same conditions.



Scheme 2. General equation of Mo-catalyzed epoxidation of cyclooctene

Complexes **1** and **5-7** are insoluble or sparingly soluble in cyclooctene at room temperature and remain undissolved at 80°C prior to the TBHP addition (orange brown slurry). However, after the addition of aqueous TBHP **1**, **6** and **7** dissolve completely in the organic phase. Complex **5** remains partially undissolved at 1% Mo loading at the beginning of the reaction, but dissolves completely within 30 min. A biphasic system consisting of a colored organic phase and a colorless aqueous phase is observed, suggesting that the oxidation catalyst is mostly confined in the organic phase. An independent miscibility investigation shows that, upon mixing aqueous TBHP and cyclooctene, TBHP is completely transferred to the organic phase. Therefore, water does not seem to play any specific role in the catalytic process.

The first catalytic experiments were performed with a 1/200/100 Mo/TBHP/cyclooctene molar proportion. The results (Table 3) and the time profile of the conversion (Figure 2) show that the cyclooctene conversion is faster in the order **1** > **5** > **6** ~ **7**. The reference complex **1** is the most efficient precatalyst, yielding a nearly quantitative conversion in 5.5 h. Half of the cyclooctene was consumed in 10 minutes in the presence of **1**, whereas 70 min were necessary to convert the same amount in the presence of **5**, which is the next most active pre-catalyst. However, the selectivity was much better for **5** (97%, vs. 89% for **1**). A similar behaviour was previously reported for the oleic acid epoxidation by cumene hydroperoxide (60.1% selectivity with  $[\text{MoO}_2(\text{SAP})(\text{EtOH})]$  vs. 50.3% with  $[\text{MoO}_2(\text{acac})_2]$ ).<sup>[52]</sup> No conversion was

obtained in the presence of the ligand SAPH<sub>2</sub> alone. The results obtained with compound **5**, even though without solvent and using aqueous TBHP, are competitive with respect to the state of the art (see Table S1 in the SI). Note the slight inflection of the conversion curve for compound **5**, indicating the presence of an induction phenomenon. This may be related to solubility issues (cf. results at different catalyst concentration, below). The presence of an induction time in catalyzed olefin epoxidation by TBHP has also been reported for other Mo<sup>VI</sup> catalyts.<sup>[67]</sup>

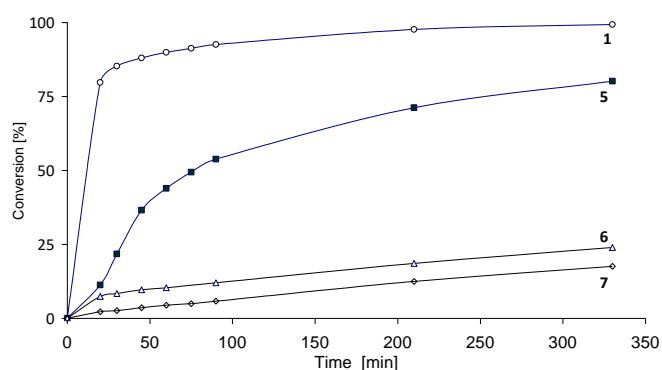


Figure 2. Cyclooctene conversion vs. time with  $[\text{MoO}_2(\text{acac})_2]$  (**1**) and different dinuclear precatalysts  $[\text{MoO}_2\text{L}_2]$  (**5-7**) at 80°C.

Table 3. Results of the cyclooctene epoxidation catalysis experiments.<sup>[a]</sup>

Catalyst	T(°C)	TOF/h <sup>-1</sup> [b]	TON[c]	Conv/%	Yield/%	Select/%
<b>1</b>	80	305	97 (86)	99	88	89
<b>5</b>	80	56	79 (77)	80	78	98
<b>5</b>	50	14	24 (23)	23	22	97
<b>7</b>	80	28	23 (20)	18	16	88
<b>6</b>	80	43	17 (15)	24	22	90

[a] Conditions: Mo/TBHP/cyclooctene = 1 :200 :100; t = 5.5 h. [b] calculated on the time interval with maximum slope for the conversion plot (see text). [c] converted cyclooctene (cyclooctene oxide formed) after 5.5 h.

The efficiency of the different dinuclear precatalysts is at least in part related to their stability under catalytic conditions. The <sup>1</sup>H NMR analysis in d<sup>6</sup>-DMSO of the final solution led the identification of complex  $[\text{MoO}_2\text{L}(\text{DMSO})]$  as the only ligand-containing species when using compound **5** (L= SAP). Notably, neither SAPH<sub>2</sub> nor hydrolysis products (such as salicylaldehyde) were visible in the spectrum. The same conclusion was already reported for  $[\text{MoO}_2(\text{SAP})(\text{D})]$  and  $[\text{MoO}_2(\text{SAP})_2]$  complexes used in organic solvents.<sup>[50, 53, 68-69]</sup> Our results show that this holds true in the presence of water. When L= SAE or SAMP, on the other hand, ligand hydrolysis and complex decomposition were deduced by the presence of signals unambiguously assigned to salicylaldehyde. Therefore, the structure of the SAP ligand is crucial for the reaction selectivity as well as for the stability of the

“MoO<sub>2</sub>L” moiety under these experimental conditions. Further investigations were therefore confined to the SAP system.

The catalytic efficiency of complex **5** was probed by progressively decreasing the catalyst loading of from 1% to 0.1% (results in Table 4 and Figure 3). The most important remark is that the turnover frequency is not invariant with the catalyst concentration. Rather, the conversion vs. time profile remains approximately constant. Only upon going from 0.15 to 0.10% does the activity significant change (Figure 3). This suggests that only a minor portion of the Mo complex is in the catalytically active form. The selectivity remains very high, but is highest (>90%) for a Mo loading of  $\geq 0.6\%$ . No induction time was discernible in these experiments.

Mo loading	TOF/h <sup>-1</sup> [b]	TON <sup>[c]</sup>	Conv/%	Select/%
<b>0.1</b>	131	503	50	84
<b>0.15</b>	203	195	60	75
<b>0.23</b>	123	269	63	80
<b>0.33</b>	104	196	65	83
<b>0.6</b>	42	111	67	91
<b>1.0</b>	44	65	65	93

[a] Conditions: TBHP/cyclooctene = 200 :100; t = 4 h; T = 80°C. [b] calculated on the time interval with maximum slope for the conversion plot (see text). [c] converted cyclooctene after 4h.

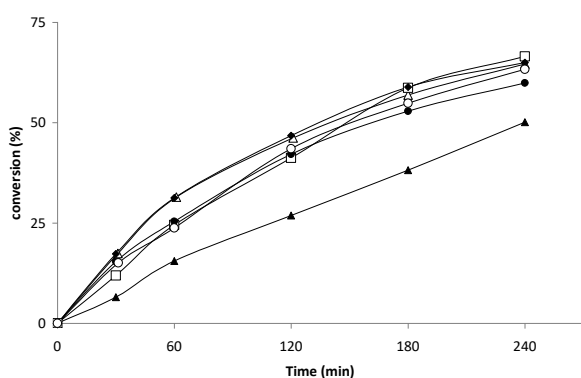


Figure 3. Conversion of cyclooctene versus time for different Mo/cyclooctene ratio with [MoO<sub>2</sub>(SAP)<sub>2</sub>] (**5**) (0.10% (▲), 0.15% (●), 0.23% (○), 0.33% (◆), 0.60% (□), 1.00% (△)). The reaction conditions are given in Table 4 (T = 80°C).

The reaction with complex **5** was also tested at a lower temperature (50°C), in order to verify the temperature dependence of the activity and selectivity. The selectivity remained high at both temperatures (Table 3). The activity dropped dramatically and a significant induction time was now observed (see figure S4 in SI). This could be rationalized by the longer time needed to activate the precatalyst, although the

reduced catalyst solubility at the lower temperature may also contribute to this difference.

Since complex **5** showed the best activity and stability among the different [MoO<sub>2</sub>L]<sub>2</sub> complexes, its methanol-stabilized mononuclear derivative **2** was also investigated under the same conditions at different catalyst loadings (see Table 5 and Figure 4). Like with complex **5**, the activity did not drop significantly upon lowering the catalyst concentration and the presence of an induction phase was apparent in some cases. The activity of **2** is only marginally lower than that of **5** under the same conditions (*cf.* Table 3 for the result with 1% Mo loading). The selectivities are also essentially identical. Hence, we suppose that both precatalysts are ultimately generating the same active species.

Mo loading	TOF/h <sup>-1</sup> [b]	TON <sup>[c]</sup>	Conv/%	Select/%
<b>0.05</b>	1460	2058	50	72
<b>0.10</b>	529	896	51	81
<b>0.25</b>	387	423	67	88
<b>1.0</b>	39	79	79	93

[a] Conditions: TBHP/cyclooctene = 200 :100; t = 3 h; T = 80°C. [b] calculated on the time interval with maximum slope for the conversion plot (see text). [c] converted cyclooctene after 3h.

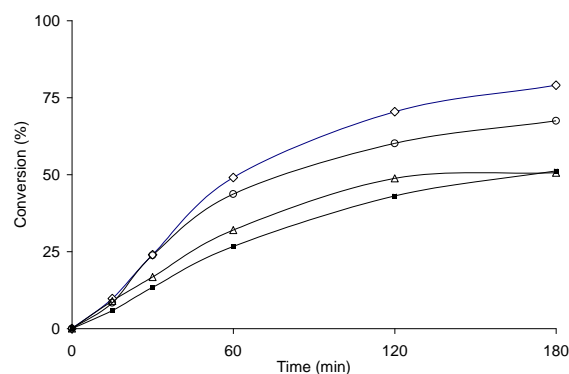


Figure 4. Conversion of cyclooctene versus time for [MoO<sub>2</sub>(SAP)(MeOH)] (**2**) at various Mo loadings (0.05% (△), 0.10% (■), 0.50% (○), 1.00% (◇)). The reaction conditions are given in Table 5.

Since compounds **2** and **5** are related to each other by facile loss/addition of MeOH, experiments were also run with compound **5** as catalyst in the presence of added methanol. These experiments were carried out at 0.6% loading and at various MeOH/Mo ratios (see Table 6 and Figure 5). The experiment run with MeOH/Mo = 1 corresponds to the same stoichiometry as the experiment run with catalyst **2**. Contrary to the experiments run with isolated **2**, no clear induction phase was visible under these conditions. The results show once again similar activities and selectivities to those obtained with the isolated compounds **2** and **5** under the same conditions. Furthermore, addition of excess

MeOH has little effect on the catalytic activity, showing at best a marginal decrease of activity for the highest MeOH/Mo ratios. All these results show that the presence of MeOH is not necessary to generate the active catalyst but at the same time it does not have a negative effect on the catalytic cycle.

MeOH/Mo <sup>(a)</sup>	T(°C)	TOF/h <sup>-1(b)</sup>	TON <sup>(c)</sup>	Conv/%	Select/%
1	80	94	139	84	80
5	80	83	117	71	77
10	80	61	116	70	84
30	80	57	114	69	80

[a] Conditions: Mo/TBHP/cyclooctene = 0.6 :200 :100; T = 80°C; t = 4 h. [b] calculated on the time interval with maximum slope for the conversion plot (see text). [c] converted cyclooctene (cyclooctene oxide formed).

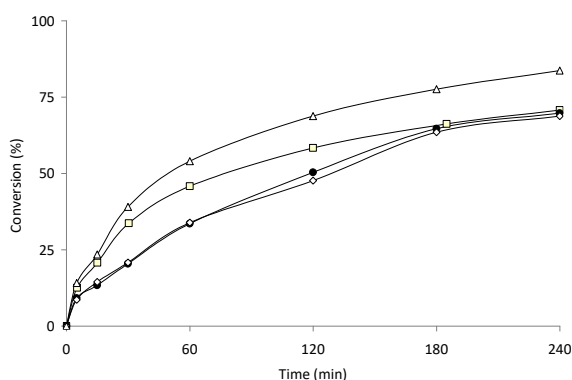


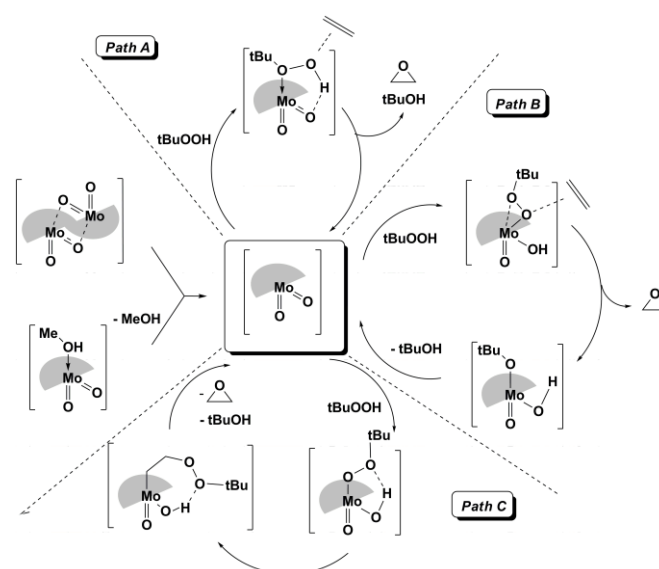
Figure 5. Conversion of cyclooctene versus time with different MeOH/Mo ratio MeOH/Mo = 1 ( $\Delta$ ), 5 ( $\square$ ), 10 ( $\bullet$ ), 30 ( $\diamond$ ). The reaction conditions are given in Table 6.

To summarize, the catalysis experiments reported here have yielded the following information: (i)  $[\text{MoO}_2(\text{SAP})]_2$  and  $[\text{MoO}_2(\text{SAP})(\text{MeOH})]$  yield essentially the same activity and selectivity; (ii) the selectivity for  $[\text{MoO}_2(\text{SAP})]_2$  is nearly the same at 50 and 80°C; (iii) both precatalysts probably generate the same active species; (iv) only a minor amount of the Mo complex is present in the active form; (v) water appears to have a negative effect on the catalysis for the SAE and SAMP systems, notably by favouring the ligand hydrolytic degradation, whereas the SAP-containing catalyst appears to survive under the reaction conditions.

### 3. Mechanistic considerations and DFT calculation.

Although there is general consensus on the notion that the catalyst first activates the oxidant molecule followed by oxygen atom transfer to the substrate,<sup>[67, 70-76]</sup> there is no uniform agreement on the details of the oxidant activation and oxygen atom transfer. As stated in the introduction, the ONO system of

interest here has the particular feature of easily liberating a coordination site by dimer splitting or alcohol dissociation, yielding a 5-coordinate  $[\text{MoO}_2\text{L}]$  intermediate to which the oxidant may also coordinate as a neutral molecule. A pathway that involves coordination of the TBHP oxidant as a neutral molecule, with possible assistance of a  $\text{OH}\cdots\text{O}$  hydrogen bond, has been proposed for this system (cycle **A** in Scheme 3).<sup>[52-54]</sup> To the best of our knowledge, this mechanism has not yet been probed by computational investigations. The more typical pathways proposed for the oxygen transfer to olefin by dioxomolybdenum(VI) catalysts (all of them being pseudo-6-coordinated systems) involve the activation of TBHP by proton transfer to an oxido ( $\text{Mo}=\text{O}$ ) or peroxido  $[\text{Mo}(\text{O}_2)]$  function to yield a pseudo-7-coordinate  $\text{Mo}(\text{OH})(\text{OO}t\text{Bu})$  [or  $\text{Mo}(\text{OOH})(\text{OO}t\text{Bu})$ ] intermediate. For the 5-coordinate  $\text{MoO}_2(\text{SAP})$  system under consideration here, and without consideration of the involvement of peroxide functions which were not spectroscopically detected at the end of the catalysis, this possibility would result in 6-coordinate  $\text{Mo}(\text{OH})(\text{OO}t\text{Bu})$  intermediates (cycles **B** and **C**).<sup>[72-74]</sup>



Scheme 3. Schematic summary of olefin epoxidation mechanisms proposed in the literature (see text) and how they could be accessed from a  $[\text{MoO}_2(\text{SAP})]_2$  or  $[\text{MoO}_2(\text{SAP})(\text{MeOH})]$  pre-catalyst. The ligands are omitted and the olefin is simplified with ethylene for clarity.

In terms of the subsequent O atom transfer step, path **A** was proposed to continue with an exogenous nucleophilic attack of the  $\text{O}^\alpha$  atom by the olefin, which therefore does not directly interact with the metal center, concomitant with transfer of the oxidant proton to the oxido ligand and formation of  $\text{OH}$  and  $\text{O}t\text{Bu}$  ligands (we use a nomenclature where atom  $\text{O}^\alpha$  binds the H atom in TBHP or the Mo atom in the *tert*-butylperoxido complex, whereas atom  $\text{O}^\beta$  is the atom bearing the *tert*-Bu group:  $\text{Mo}-\text{O}^\alpha-\text{O}^\beta-t\text{Bu}$ ,  $\text{H}-\text{O}^\alpha-\text{O}^\beta-t\text{Bu}$ ). Cycle **B** continues with the same attack of the  $\text{O}^\alpha$  atom, assisted by an incipient interaction between the  $\text{O}^\beta$  atom and the metal, the subsequent steps being identical to those of cycle **A**.<sup>[67, 70-71, 74]</sup> According to this view, the incipient  $\text{Mo}-\text{O}^\beta$  interaction activates the  $\text{O}^\alpha$  atom towards the nucleophilic attack.<sup>[77-78]</sup> In cycle **C**, on the other hand, the olefin inserts into the  $\text{Mo}-\text{O}^\alpha$  bond (possibly by prior metal coordination) and forms an organometallic intermediate, which then evolves by ring closure, with assistance by a  $\text{OH}\cdots\text{O}^\beta$  interaction, and simultaneous elimination of the epoxide and  $t\text{BuOH}$ .<sup>[72-73]</sup> In the

latter mechanism, the oxido ligand used to borrow the oxidant proton is directly regenerated, whereas cycles **A** and **B** yield an intermediate  $\text{Mo}(\text{OH})(\text{O}^{\beta}\text{Bu})$  species which must subsequently eliminate  $t\text{BuOH}$  to regenerate the oxido species. One common point of all these mechanistic proposals is transfer of the  $\text{O}^{\alpha}$  atom to the olefin while the  $\text{O}^{\beta}$  atom ends up in the  $t\text{BuOH}$  by-product, in agreement with the experimental evidence. Cycles **B** and **C** may be seen as the natural extension of the original mechanisms proposed by Sharpless<sup>[79]</sup> and Mimoun,<sup>[80]</sup> with the *tert*-butylperoxido moiety  $\text{MoOO}t\text{Bu}$  replacing the peroxido moiety  $\text{Mo}(\text{O}_2)$ . We decided to probe the likelihood of these three mechanisms for the  $[\text{MoO}_2(\text{SAP})]$  system.

In previous computational investigations, it was shown that (pseudo)octahedral  $\text{LMoO}_2$  systems are able to activate ROOH by proton transfer, since a  $\text{Mo}=\text{O}$  moiety can redistribute its  $\pi$  electron density to yield  $\text{Mo}(\text{OH})(\text{OOR})$  with the same number of valence electron and a coordination number increased by one unit. No coordination of TBHP as a neutral ligand was highlighted. For the present catalytic system, fragmentation of the dinuclear compound **5** yields two mononuclear pentacoordinated “ $\text{MoO}_2(\text{SAP})$ ” species, identical to the product of MeOH dissociation from **2**. Our system is therefore electronically less saturated and potentially more reactive. The very similar catalytic activity of **2** and **5** and the negligible effect of an excess of MeOH are in agreement with weak MeOH coordination to the active species, which agrees with the long Mo-O bond observed in the X-ray structures of  $[\text{MoO}_2(\text{SAP})(\text{EtOH})]$  (2.370(3) Å).<sup>[39]</sup> On the basis of the above experimental evidence, we shall assume that the active form of our catalyst is  $[\text{MoO}_2(\text{SAP})]$ .

Hence, using a DFT approach, we started with the energetic assessment of  $[\text{MoO}_2(\text{SAP})]$  relative to the dinuclear compound **5**, the MeOH adduct **2**, the two types of activated TBHP complexes – the  $[\text{MoO}_2(\text{SAP})(t\text{BuOOH})]$  adduct of cycle **A** and the  $[\text{MoO}(\text{OH})(\text{SAP})(\text{OO}t\text{Bu})]$  intermediates of cycles **B** and **C** – and finally the adduct resulting from addition of the  $t\text{BuOH}$  by-product (see Figure 6). Comparison of the optimized geometries of  $[\text{MoO}_2(\text{SAP})(\text{L})]$  (L = MeOH,  $t\text{BuOH}$ ) with that experimentally available for L = EtOH<sup>[39]</sup> and the optimized geometry of **5** with that experimentally available for **6**<sup>[62]</sup> (details in the Supporting Information table S2) verifies the suitability of the selected computational level.

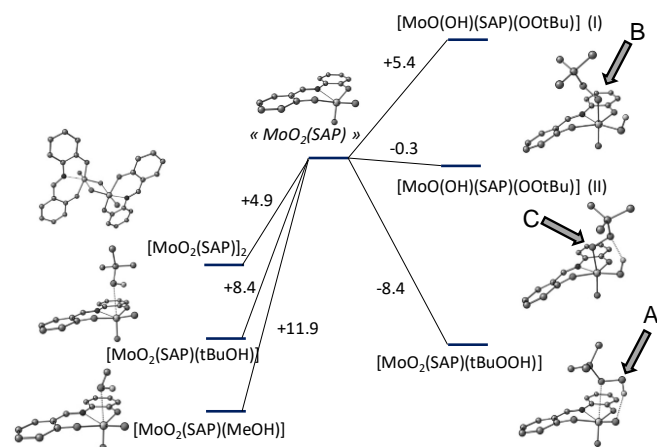


Figure 6. Relative energies ( $\Delta\text{H}$  in kcal/mol relative to  $[\text{MoO}_2(\text{SAP})] + \text{TBHP} + \text{C}_2\text{H}_4$ ) and optimized geometries for compounds implicated in epoxidation by TBHP catalyzed by compounds **2** and **5**. The arrows indicate the position of

olefin attack according to the cycles **A**, **B** and **C** of Scheme 3. C-bonded hydrogen atoms have been omitted for clarity.

The most stable species is **2**, followed by the  $t\text{BuOH}$  adduct. The energetic preference for MeOH relative to  $t\text{BuOH}$  may be due to steric bulk, as suggested by the lengthened Mo-O distance (2.68 vs. 2.56 Å). Note that these distances are quite long, as expected from the strong *trans* stabilizing effect of the oxido ligand. Alcohol coordination is assisted by a H-bond, the alcohol OH group being the proton donor and the equatorial oxido ligand the acceptor ( $\text{H}\cdots\text{O} = 2.321$  Å for MeOH; 2.216 Å for  $t\text{BuOH}$ ). The presence of this interaction is also suggested by the very small Mo-O-H angle ( $92.1^\circ$  for MeOH,  $86.0^\circ$  for  $t\text{BuOH}$ ), whereas the Mo-O-R angles are much larger ( $125.2^\circ$  for Me,  $145.0^\circ$  for  $t\text{Bu}$ ) and by the OH bond eclipsing the Mo=O bond (the dihedral O-Mo-O-H angle is  $4.6^\circ$  for both alcohols). Both adducts are more stable than the dimer **5**, which is in turn slightly more stable than the 5-coordinate  $[\text{MoO}_2(\text{SAP})]$  monomer. However, the calculated enthalpies ( $\Delta\text{H}_{298}$ ) involved for the dimer splitting (4.9 Kcal/mol) or for the MeOH release (11.9 Kcal/mol) are relatively small, consistent with these processes being fast and reversible on the timescale of the catalytic cycle. It is also worth noting that the existence of a monomeric  $[\text{MoO}_2\text{L}]$  in the solid state as a metastable intermediate, during the thermal conversion of a specific  $[\text{MoO}_2\text{L}(\text{MeOH})]$  polymorph to  $[\text{MoO}_2\text{L}]_n$ , has recently been described ( $\text{H}_2\text{L} = \text{N-Salicylidene-2-amino-3-hydroxypyridine}$ , closely related to  $\text{H}_2\text{SAP}$ ).<sup>[81]</sup>

As expected, the  $[\text{MoO}_2(\text{SAP})(t\text{BuOOH})]$  adduct of cycle **A** is stabilized by a H bond between the TBHP  $\text{O}^{\alpha}$  atom as proton donor and the equatorial oxido ligand as proton acceptor. However, in spite of such strong stabilization ( $\text{H}\cdots\text{O} = 1.870$  Å), this system has essentially the same energy as the  $t\text{BuOH}$  adduct relative to the  $[\text{MoO}_2(\text{SAP})]$  monomer. This is explained by a very weak metal binding. The angular requirement to optimize the H-bond, which must obviously be the driving force to the formation of this adduct, constrains the  $\text{O}^{\beta}$  atom to remain quite far from the Mo center ( $> 3$  Å), although well positioned on the axial site for overlap with the metal accepting orbital. This geometrical feature highlights once again the weak bonding of neutral ligands to the 5-coordinate  $\text{MoO}_2\text{L}$  species in the position *trans* to an oxido ligands. Note however, that the  $\text{O}^{\beta}$  atom positioning is important for the incipient bond formation in the follow-up of cycle **A** (*vide infra*).

For the  $[\text{MoO}(\text{OH})(\text{SAP})(\text{OO}t\text{Bu})]$  system, two local minima were calculated, one (II) stabilized by a strong  $\text{O}^{\beta}\cdots\text{HO}$  hydrogen bond (1.789 Å), serving as intermediate for cycle **C**, the other one (I) without any H-bond stabilization, serving as intermediate for cycle **B**. Contrary to a previous investigation of the catalytic system  $[\text{Cp}^*\text{MoO}(\text{OH})\text{Cl}(\text{OO}t\text{Bu})]$ ,<sup>[74]</sup> there is no significant  $\text{Mo}\cdots\text{O}^{\beta}$  interaction in this case ( $> 2.9$  Å;  $\text{Mo}-\text{O}^{\alpha}-\text{O}^{\beta} = 112.6^\circ$ ).

After the location of all reasonable reaction intermediates, the olefin approach was investigated using  $\text{C}_2\text{H}_4$  as model substrate, as indicated by the blue arrows in Figure 6. The energetic profiles of the three cycles are illustrated in Figure 7, whereas the geometry of each cycle key transition state is illustrated in Figure 8. For cycle **A**, attack of the  $\text{O}^{\alpha}$  atom of intermediate  $[\text{MoO}_2(\text{SAP})(t\text{BuOOH})]$  led to formation and release of the epoxide product, concomitant with the formation of  $[\text{MoO}(\text{OH})(\text{O}^{\beta}\text{Bu})(\text{SAP})]$ . The transformation is exothermic by -37.4 kcal/mol relative to  $\{[\text{MoO}_2(\text{SAP})] + \text{TBHP} + \text{C}_2\text{H}_4$  and

the transition state  $TS_A$  is located at 14.1 kcal/mol on the same scale (22.5 kcal/mol from  $\{[MoO_2(SAP)(tBuOOH)] + C_2H_4\}$ ). The geometry of  $TS_A$  shows a rather advanced stage of atom transfer, with the  $O^\alpha$  atom already significantly departed from the  $O^\beta$  atom ( $O^\alpha \cdots O^\beta = 1.89 \text{ \AA}$ ) and relatively close to the olefin moiety ( $O^\alpha \cdots C = 1.83$  and  $2.18 \text{ \AA}$ ), while the olefin  $C=C$  bond has slightly lengthened to  $1.379 \text{ \AA}$ . Formation of the  $Mo-O^\beta$  interaction is already well on its way ( $2.39 \text{ \AA}$ , vs.  $1.944 \text{ \AA}$  in the final product). On the other hand, the TBHP H atom is still relatively close to the  $O^\alpha$  atom ( $1.00 \text{ \AA}$ ) and far from its final oxido ligand destination ( $1.67 \text{ \AA}$ ).

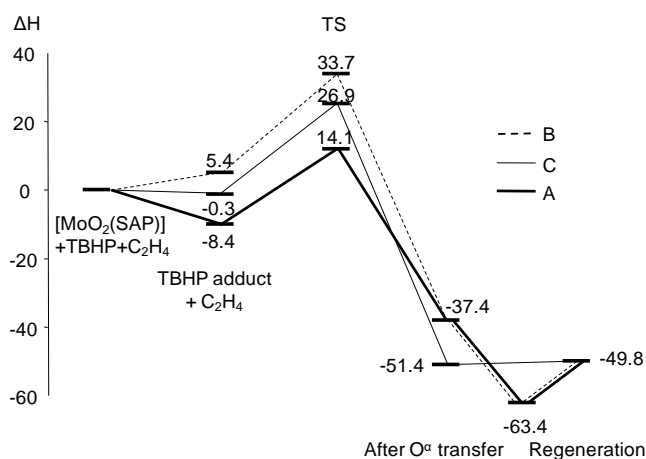


Figure 7. Energetic profiles ( $\Delta H$  in kcal/mol relative to  $[MoO_2(SAP)] + TBHP + C_2H_4$ ) for catalytic cycles **A**, **B**, **C** of Scheme 3.

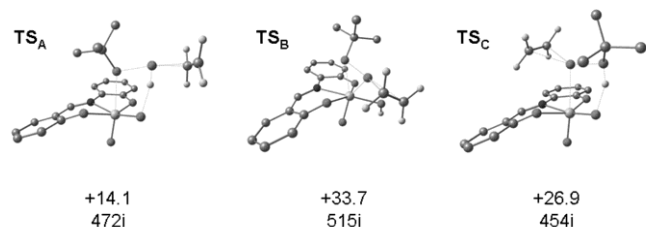


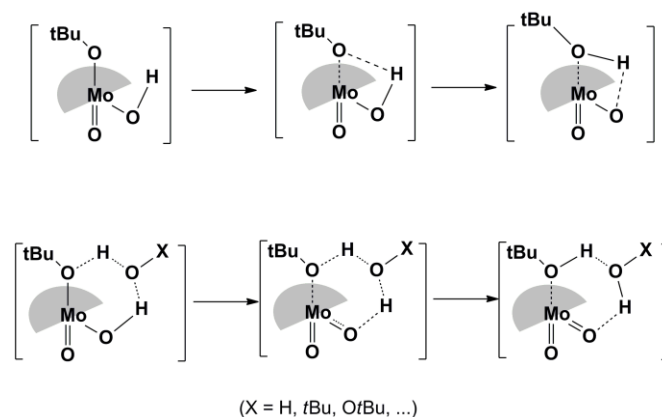
Figure 8. Optimized geometries, relative energies ( $\Delta H$  in kcal/mol relative to  $[MoO_2(SAP)] + TBHP + C_2H_4$ ), and imaginary frequency ( $cm^{-1}$ ) of the transition states for the three pathways **A**, **B** and **C** considered in Scheme 3.

The olefin approaches through paths **B** and **C** were found to have higher activation barriers (33.7 and 26.9 Kcal/mol for  $TS_B$  and  $TS_C$ , respectively). Path **B**, starting from  $[MoO(OH)(SAP)(OOtBu)]-I$ , leads to the same  $[MoO(OH)(OtBu)(SAP)]$  intermediate as path **A**. The transition state  $TS_B$  that connects these two states, like  $TS_A$ , shows a significantly weakened  $O^\alpha \cdots O^\beta$  interaction ( $1.85 \text{ \AA}$ ), the olefin proximity ( $O^\alpha \cdots C = 1.89$  and  $2.23 \text{ \AA}$ ), and olefin  $C=C$  bond lengthening ( $1.368 \text{ \AA}$ ). The  $O^\alpha$  atom has slightly departed from the Mo center ( $2.10 \text{ \AA}$ , vs.  $2.05 \text{ \AA}$  in the starting  $[MoO(OH)(SAP)(OOtBu)]-I$ ), whereas the  $O^\beta$  is already close to the  $Mo-O$  distance in the final product ( $2.15 \text{ \AA}$ ).

Path **C** led to a surprising outcome. Instead of the expected insertion of the olefin into the  $Mo-O$  bond, as reported for the organometallic system  $[CpMoO(OH)(CH_3)(OOCCH_3)]^{[73]}$  and also for the  $[MoO(OH)Br_2(MeN=CH-CH=NMe)(OOME)]$  model system  $^{[72]}$  (in spite of several attempts this path could not be located) the

olefin approach smoothly resulted in  $O^\alpha$  atom transfer to the olefin and direct elimination of  $tBuOH$  with epoxide trapping by the metal center, to yield the adduct  $[MoO_2(SAP)(OC_2H_4)]$ , in a single elementary step. In the transition state  $TS_C$  of this step, the positioning of the  $O^\alpha$  atom relative to  $O^\beta$  and the olefin is similar to those observed in  $TS_A$  and  $TS_B$  ( $O^\alpha \cdots O^\beta = 1.76 \text{ \AA}$ ,  $O^\alpha \cdots C = 2.14$  and  $2.30 \text{ \AA}$ ,  $C-C = 1.352 \text{ \AA}$ ) while the proton that originated from the  $O^\alpha$  atom of the TBHP reagent, temporarily located on the hydroxido ligand in the  $[MoO(OH)(SAP)(OOtBu)]-II$  intermediate, has already jumped back onto the  $O^\beta$  atom ( $1.00 \text{ \AA}$ ) to form the  $tBuOH$  by-product. The  $Mo-O^\alpha$  interaction is significantly weakened in this transition state ( $2.61 \text{ \AA}$ ), before strengthening again in the final product ( $2.52 \text{ \AA}$ ). The combination of  $[MoO_2(SAP)(OC_2H_4)]$  and  $tBuOH$  is located at  $-51.4$  kcal/mol on the scale of Figure 7 and is thus thermodynamically favored by  $14.0$  kcal/mol relative to the combination of  $[MoO(OH)(OtBu)(SAP)]$  and free  $C_2H_4O$  that forms in cycles **A** and **B**.

In order to complete the catalytic cycle, we must now examine how the complexes that have been obtained,  $[MoO(OH)(OtBu)(SAP)]$  from paths **A** and **B** and  $[MoO_2(SAP)(OC_2H_4)]$  from path **C** can regenerate the starting point of each respective cycle. Complex  $[MoO(OH)(OtBu)(SAP)]$  can intramolecularly transfer a proton from the OH ligand to the OtBu ligand as shown in Scheme 4 to yield  $[MoO_2(SAP)(tBuOH)]$  (exothermic by  $12.4$  kcal/mol) followed by  $tBuOH$  dissociation. Intramolecular proton transfer processes of this type have been calculated for other systems and were generally found to proceed with very high barriers in the gas phase (e.g.  $43.9$  kcal/mol for converting  $[Cp^*MoO(OH)_2]^+$  to  $[Cp^*MoO_2(OH_2)]^+$ ) $^{[82]}$  because of needed angular distortions to approach the proton donor and acceptor ligands. These barriers were shown to dramatically drop, however, in the presence of proton shuttle molecules, such as water or alcohols (in the cited example, the barrier dropped from  $43.9$  to  $10.3$  kcal/mol by the introduction of one water molecule and to zero in the presence of two water molecules). $^{[82]}$  For the solvent-free catalytic system investigated here, as discussed previously, water should be excluded from the organic phase that contains the substrate, the epoxide product, and the catalyst. However, the TBHP reagent and the  $tBuOH$  product, which are also confined in the organic phase, can equally serve as proton shuttle (Scheme 4). Therefore, this step is not expected to introduce a rate limiting barrier in the catalytic cycle. From the product of path **C**,  $[MoO_2(SAP)(OC_2H_4)]$ , the catalyst regeneration is in principle even simpler, needing only dissociation of the epoxide product.

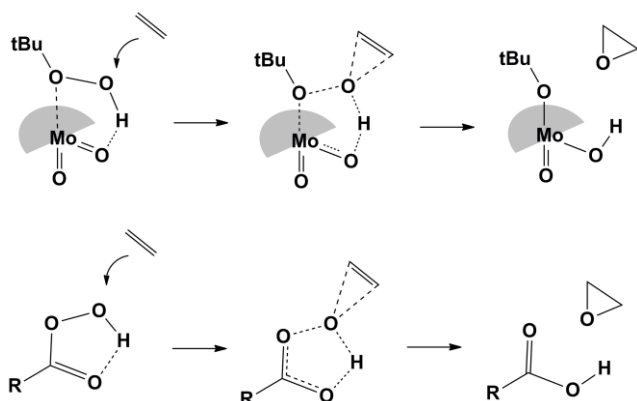


Scheme 4. Proton shuttle effect on the catalyst reactivation for paths **A** and **B**.

Note that epoxide coordination to  $[\text{MoO}_2(\text{SAP})]$  provides a slightly better stabilization (-10.0 kcal/mol) than  $t\text{BuOH}$  coordination (-8.4 kcal/mol), whereas  $[\text{MoO}(\text{OH})(\text{OtBu})(\text{SAP})]$  is endothermic relative to  $[\text{MoO}_2(\text{SAP})]$  and  $t\text{BuOH}$  by +4.0 kcal/mol. It is also possible to envisage alternative reactivation processes, without the need to go through the 5-coordinated  $[\text{MoO}_2(\text{SAP})]$  intermediate. For instance, direct addition of a new TBHP molecule to  $[\text{MoO}(\text{OH})(\text{OtBu})(\text{SAP})]$  could lead to proton transfer to the  $t\text{BuO}$  ligand and  $t\text{BuOH}$  expulsion, either directly or via the second  $\text{Mo}=\text{O}$  function, generating  $[\text{MoO}(\text{OH})(\text{SAP})(\text{OO}t\text{Bu})]$  or  $[\text{MoO}_2(\text{SAP})(\text{TBHP})]$ . However, these processes should also in principle occur with relatively low activation barriers with respect to that of the oxygen transfer step, which is therefore the rate-determining step of the catalytic cycle.

The resting state of cycles **A** and **B**<sup>[83]</sup> is the  $t\text{BuOH}$  adduct and that of cycle **C** is the epoxide adduct when the catalysis is operated with compound **5**. However, because of the fast ligand exchange equilibria, the slightly more stable epoxide adduct could be considered as the common resting state for all cycles. When the catalysis is operated with **2** or with **5/MeOH**, the lowest energy species (and catalyst resting state) is the  $\text{MeOH}$  adduct. Note, however, that when entropic considerations are taken into account (e.g. on a Gibbs free energy scale), the rate determining intermediate may become the 5-coordinate  $[\text{MoO}_2(\text{SAP})]$ . The accurate calculation of free energies in condensed phases is haunted by many problems and therefore we shall restrict our considerations to the enthalpy differences. The analysis of the above computational results leads to the conclusion that the lowest energy pathway for the olefin epoxidation with TBHP catalyzed by the  $[\text{MoO}_2(\text{SAP})]$  system is cycle **A**.

The interesting feature of this new mechanistic scenario is the lack of apparent TBHP activation in the ground state. The TBHP molecule is relatively undistorted in the  $[\text{MoO}_2(\text{SAP})(\text{TBHP})]$  adduct with an unstrained  $\text{O}^\beta\text{-O}^\alpha\text{-H}$  angle. A strain on this angle, on the other hand, occurs en route toward the transition state, caused by the attraction of the  $\text{O}^\beta$  atom during the establishment of the incipient  $\text{Mo}-\text{O}^\beta$  bond. This activation method may be related to the effect of the carbonyl group of peracids in Bartlett's epoxidation,<sup>[84]</sup> where a strain of the same angle is induced during the proton transfer in the 5-membered ring that accompanies the oxygen atom attack by the olefin.<sup>[85-87]</sup> The two pathways are schematically compared in Scheme 5. Whereas in Bartlett's mechanism, the strain at the  $\text{O}-\text{O}-\text{H}$  angle is mostly due to the H-bonding interaction and intramolecular proton transfer, in path **A** of the  $[\text{MoO}_2(\text{SAP})]$ -catalyzed oxidation by TBHP, both H-bonding and  $\text{Mo}\cdots\text{O}^\beta$  interactions, leading to proton transfer and  $\text{Mo}-\text{O}^\beta$  bond formation, contribute to the activation.



Scheme 5. Comparison of oxygen transfer pathways to olefin by peracids and  $[\text{MoO}_2(\text{SAP})]$ -coordinated TBHP.

## Conclusion

We have shown here for the first time that  $[\text{MoO}_2(\text{SAP})]_2$  is able to act as a pre-catalyst in a solvent-free process using aqueous TBHP. Contrary to suggestions that " $\mu$ -oxo dimeric complexes lead to irreversible catalyst deactivation",<sup>[55-56]</sup> the  $\mu$ -oxo dimeric SAP derivative serves indeed as a stable, long shelf life, convenient reversible source of 5-coordinate  $[\text{MoO}_2(\text{SAP})]$  with the same activity as that provided by the methanol adduct **2**. In agreement with previous related studies, which focused on the use of alcohol adducts in organic solvents, this system shows a high activity and a high selectivity towards the epoxidation product. The computational investigation highlights a unique feature of this "5-coordinate" catalytic system, which is capable of activating the TBHP oxidant through a simple adduct formation, benefitting from the combined action of a hydrogen bond and a weak  $\text{Mo}\cdots\text{O}^\beta$  interaction. The ring strain in the resulting 5-membered cycle at the level of the transition state helps reduce the O-atom transfer barrier. The resulting mechanism (cycle **A** of Scheme 3) is closely related to the classical Bartlett's mechanism for the stoichiometric epoxidation with peracids. The results of this study points towards the power of 5-coordinate  $[\text{MoO}_2\text{L}]$  structures in terms of efficient epoxidation catalysis. It is also conceivable that at least a few of the catalytic systems based on pseudo-6-coordinate  $[\text{MoO}_2\text{L}]$  complexes, for which cycles **B** and **C** have been proposed, might in fact operate through cycle **A** after prior partial decoordination of the chelating ligand.

## Experimental Section

### Materials and methods

All preparations were carried out in air. Water was deionised twice before use. Organic solvents (ethanol, diethylether) and organic compounds (2-hydroxybenzaldehyde, 2-aminoethanol, 2-aminophenol, 2-aminomethylpropanol) were employed as received without any purification.  $[\text{MoO}_2(\text{acac})_2]$  (**1**) was synthesized as previously described<sup>[88]</sup> and used freshly prepared. Cyclooctene (98% Aldrich), cyclooctene oxide and TBHP (70% in water, ACROS) were used as received. The thermogravimetric analyses were performed on a SETARAM TGA 92-16.18 thermal analyzer. The sample was placed into a nickel/platinum alloy crucible and heated at  $0.83 \text{ K s}^{-1}$  in a reconstituted air flow from  $15^\circ\text{C}$  to  $600^\circ\text{C}$ . An empty crucible was used as a reference. Infrared spectra were recorded in KBr matrices at room temperature with a Mattson Genesis II FTIR spectrometer.  $^1\text{H}$  spectra were recorded at 200.1 MHz on a Bruker Avance DPX-200 spectrometer. Catalytic reactions were followed by gas chromatography on an Agilent 6890A chromatograph equipped with FID detector, a HP5-MS capillary column (0.30 m x 0.25 mm x 0.25 m) and automatic sampling, or on a Fisons GC 8000 chromatograph equipped with FID detector and with a SPB-5 capillary column (30 m x 0.32 mm x 0.25 m). The GC parameters were quantified with authentic samples of the reactants and products. The conversion of *cis*-cyclooctene and the formation of cyclooctene oxide were calculated from calibration curves ( $r^2 = 0.999$ ) relatively to an internal standard.

**Synthesis of  $\text{SAPH}_2$  in water.** In a 100 mL Erlenmeyer flask, 1.1 mL (10.5 mmol) of 2-hydroxybenzaldehyde were added to 15 mL of distilled water. 2-Aminophenol (1.08 g 9.87 mmol) was added dropwise. The mixture was left under magnetic stirring for four hours until the product formed as an orange-red precipitate and the solution

remained colorless. The precipitate was filtered, washed with water, recrystallized from boiling ethanol and filtered again, then washed with diethylether and dried under vacuum at room temperature to give an orange microcrystalline powder. Yield 1.66 g (78.6 %). IR (KBr,  $\nu(\text{cm}^{-1})$ ): 1632 (C=N).  $^1\text{H}$  NMR (DMSO- $d_6$ ,  $\delta(\text{ppm})$ ): 6.86–7.66 (m, 8H, Ar-H), 8.99 (s, 1H, CH=N), 9.77 (s, 1H, Ar-OH), 13.82 (s, 1H, Ar-OH).

**Synthesis of SAEH<sub>2</sub> in water.** In an 100 mL Erlenmeyer flask filled with 1.1 mL (10.5 mmol) of 2-hydroxybenzaldehyde and 30 mL of distilled water, 0.6 mL (9.94 mmol) of 2-aminoethanol were added dropwise. The mixture was left under magnetic stirring for four hours, leading to a bright yellow solution. Water was eliminated under reduced pressure. The dark yellow oily residue was distilled under reduced pressure, leading to an orange oil. Yield: 1.46 g (89.0 %). IR (NaCl,  $\nu(\text{cm}^{-1})$ ): 1633 (C=N).  $^1\text{H}$  NMR(DMSO- $d_6$ ,  $\delta(\text{ppm})$ ): 3.80 (t (6Hz), 2H, CH<sub>2</sub>), 3.97 (t (6Hz), 2H, CH<sub>2</sub>), 4.81 (s, 1H, CH<sub>2</sub>OH), 6.86 - 7.49 (m, 4H, Ar-H), 8.53 (s, 1H, CH=N), 13.17 (s, 1H, Ar-OH).

**Synthesis of SAMPH<sub>2</sub> in water.** In an 100 mL Erlenmeyer flask, 1.1 mL (10.5 mmol) of 2-hydroxybenzaldehyde were added to 30 mL of water. 2-Amino-2-methylpropan-1-ol (1.01 g, 11.3 mmol) was added dropwise. The mixture was magnetically stirred for four hours and water was then eliminated under reduced pressure. The pasty orange-yellow residue was then worked out with 5 mL pentane, filtered and dried under vacuum at 50°C to give a yellow solid. Yield: 1.72 g (85.0 %). IR ( $\nu(\text{cm}^{-1})$ ): 1632 (C=N).  $^1\text{H}$  NMR(DMSO- $d_6$ ,  $\delta(\text{ppm})$ ): 1.25 (s, 6H, CH<sub>3</sub>), 4.96 (s, 1H, CH<sub>2</sub>OH), 6.82-7.50 (m, 4H, Ar-H), 8.53 (s, 1H, CH=N), 14.40 (s, 1H, Ar-OH).

**Synthesis of [MoO<sub>2</sub>(SAP).MeOH] (2) and [MoO<sub>2</sub>(SAP)]<sub>2</sub> (5).** In a 100 mL Erlenmeyer flask, 1.04 g of salicylidene aminophenol (4.90 mmol) was dissolved in 30 mL of methanol and 1.60 g of MoO<sub>2</sub>(acac)<sub>2</sub> (4.91 mmol) was added. The mixture was refluxed under magnetic stirring for 2 hours. The resulting orange precipitate was separated by filtration. The precipitate was divided in two fractions: the first one was characterized as [MoO<sub>2</sub>(SAP)(MeOH)] and a second one was dried (120°C) under reduced pressure for two hours and was characterized as [MoO<sub>2</sub>(SAP)]<sub>2</sub>. Addition of MeOH to [MoO<sub>2</sub>(SAP)]<sub>2</sub> led an immediate colour change yielding [MoO<sub>2</sub>(SAP)(MeOH)]. **[MoO<sub>2</sub>(SAP)(MeOH)] (2).** TGA (50-150°C):  $\Delta m_1 = \exp(\text{theo})$  8.5(8.6), (250 - 600°C)  $\Delta m_2 = 52.1(52.6)$ . IR (KBr,  $\nu(\text{cm}^{-1})$ ): 914 - 933 (Mo=O), 1633 (C=N). **[MoO<sub>2</sub>(SAP)]<sub>2</sub> (5)** TGA  $\Delta m = \exp(\text{theo})$  58.5 (57.6). IR (KBr,  $\nu(\text{cm}^{-1})$ ) 816 (Mo-O-Mo), 928 (Mo=O), 1633 (C=N).  $^1\text{H}$  NMR (DMSO- $d_6$ ,  $\delta(\text{ppm})$ ): 6.86 - 7.88 (m, 8H, Ar-H), 9.31 (s, 1H, CH=N). This  $^1\text{H}$  NMR spectrum in DMSO- $d_6$  is also exhibited by compound 2, suggesting that for both compounds the stable species in solution is [MoO<sub>2</sub>(SAP)(DMSO)].

**Synthesis of [MoO<sub>2</sub>(SAE)(MeOH)] (3) and [MoO<sub>2</sub>(SAE)]<sub>2</sub> (6).** In a 100 mL Erlenmeyer flask, 0.85 g (5.13 mmol) of SAEH<sub>2</sub> were dissolved in 30 mL methanol And then solid MoO<sub>2</sub>(acac)<sub>2</sub> (1.63 g, 5.00 mmol) was added. The mixture was magnetically stirred for four hours. The pale-yellow precipitate of [MoO<sub>2</sub>(SAE)(MeOH)] (3) was filtered and dried in air. Drying under reduced pressure at 120°C for two hours led to a yellow compound characterised as [MoO<sub>2</sub>(SAE)]<sub>2</sub> (6). **[MoO<sub>2</sub>(SAE)(MeOH)] (3).** TGA (50 - 150°C):  $\Delta m_1$  (%) =  $\exp(\text{theo})$  9.6(9.9),  $\Delta m_2$  (250 - 600°C) = 46.1 (45.6). IR (KBr,  $\nu(\text{cm}^{-1})$ ): 902 - 926 (Mo=O), 1639 (C=N). **[MoO<sub>2</sub>(SAE)]<sub>2</sub> (6).** TGA (250 - 600°C)  $\Delta m$  (%) =  $\exp(\text{theo})$  51.1 (50.5). IR (KBr,  $\nu(\text{cm}^{-1})$ ): 839 (Mo-O-Mo), 912 (Mo=O), 1639 (C=N).  $^1\text{H}$  NMR(DMSO- $d_6$ ,  $\delta(\text{ppm})$ ): 4.03 (t (6Hz), 2H, CH<sub>2</sub>), 4.42 (t (6Hz), 2H, CH<sub>2</sub>), 6.89 - 7.61 (m, 4H, Ar-H), 8.80 (s, 1H, CH=N).

**Synthesis of [MoO<sub>2</sub>(SAMP)(MeOH)] (4) and [MoO<sub>2</sub>(SAMP)]<sub>2</sub> (7).** In a 100 mL Erlenmeyer flask, 0.57 g (2.95 mmol) of SAMPH<sub>2</sub> were dissolved in 15 mL methanol and 0.99 g (3.04 mmol) of MoO<sub>2</sub>(acac)<sub>2</sub> were added as a solid. The mixture was magnetically stirred for one day. The resulting pale-yellow precipitate was filtered and dried in air, then redissolved in methanol and quickly filtered and dried, leading to MoO<sub>2</sub>(SAMP)(MeOH) (4). Drying under reduced pressure at 120°C for two hours led to a yellow compound characterised as

[MoO<sub>2</sub>(SAMP)]<sub>2</sub> (7). **[MoO<sub>2</sub>(SAMP)(MeOH)] (4).** TGA (50 - 150°C):  $\Delta m_1 = \exp(\text{theo})$  9.1(9.1), (250 - 600°C)  $\Delta m_2$  (%) 50.4(49.9). IR (KBr,  $\nu(\text{cm}^{-1})$ ): 911 - 929 (Mo=O), 1629 (C=N). **[MoO<sub>2</sub>(SAMP)]<sub>2</sub> (7).** TGA:  $m_i = 13.06$  mg, (250 - 600°C)  $\Delta m$  (%) 51.1(54.9). IR (KBr,  $\nu(\text{cm}^{-1})$ ): 841 (Mo-O-Mo), 928 (Mo=O), 1633 (C=N).  $^1\text{H}$  NMR ( $d_6$ -DMSO,  $\delta(\text{ppm})$ ): 1.40 (s, 6H, CH<sub>3</sub>), 4.28 (s, 2H, CH<sub>2</sub>), 6.89-7.70 (m, 4H, Ar-H), 8.68 (s, 1H, CH=N).

**Catalytic Procedure.** In a typical experiment, cyclooctene (1 equiv) and catalyst (x equiv, see tables) were mixed together then stirred in air in a round bottom flask. Dodecane or acetophenone was added as internal standard and methanol in some experiments (see tables). The reaction temperature (see Table) was regulated and then wet THBP (70% in water, 2 equiv) was added to the mixture, starting the reaction. Samples of the organic phase were periodically withdrawn. The reaction was quenched by addition of MnO<sub>2</sub>, followed by the addition of diethylether and removal of the manganese oxide and residual water by filtration through silica before GC analysis.

**Computational Details.** The geometries of all species under investigation were optimized without any symmetry constraint with the Gaussian 03 program suite.<sup>[89]</sup> The input geometries were adapted from the X-ray structures of [MoO<sub>2</sub>(SAP)(EtOH)]<sup>[39]</sup> and **6**.<sup>[62]</sup> The calculations used the standard B3LYP three-parameter functional<sup>[90-92]</sup> in conjunction with the 6-31G\*\* basis set<sup>[93-96]</sup> for C, H, N and O atoms and with the CEP-31G\* basis set<sup>[97-99]</sup> for molybdenum. The transition states were optimized using a preliminary scan of a relevant internal coordinate, followed by full optimization of the TS guided by knowledge of such coordinate. All optimized geometries were confirmed to be stationary points and local minima (for stable molecules or reaction intermediates) or first order saddle points (for the TS's) by frequency analyses. For the TS's, analysis of the imaginary frequency confirmed the expected motion along the reaction coordinate. The calculated frequencies were also used to derive the thermochemical parameters at 298 K according to the standard ideal gas approximation.

## Acknowledgements

We acknowledge the Centre National de la Recherche Scientifique (CNRS) and the Institut Universitaire de France (IUF) for financial support, the Université Paul Sabatier and its Institut Universitaire Technologique for the facilities, and the European Union for the ERASMUS mobility fellowships of J.M. and N.U. This work was granted access to the HPC resources of CINES under the allocation 2010-086343 made by GENCI (Grand Equipement National de Calcul Intensif) and to the resources of the CICT (Centre Interuniversitaire de Calcul de Toulouse, project CALMIP). S. Dejean, T. Viala, V. Martial and Y. Fauqué are acknowledged for their technical contribution within the work.

**Keywords:** Epoxidation · Molybdenum · Homogeneous Catalysis · Solvent-free · Schiff Base Ligands · DFT calculations

- [1] E. N. Jacobsen, A. Pfaltz, H. Yamamoto, *Comprehensive Asymmetric Catalysis*, Springer-Verlag, Berlin, **1999**.
- [2] I. M. Pastor, M. Yus, *Curr. Org. Chem.* **2005**, *9*, 1-29.
- [3] P. L. Matlock, W. L. Brown, N. A. Clinton, *Chem. Ind. (Dekker)* **1999**, *77*, 159-193.
- [4] Z. S. Petrovic, *Polym. Rev.* **2008**, *48*, 109-155.
- [5] T. Endo, A. Sudo, *J. Polym. Sci., Polym. Chem.* **2009**, *47*, 4847-4858.
- [6] R. N. McDonald, R. N. Steppell, J. E. Dorsey, *Org. Syn.* **1970**, *50*, 15-18.
- [7] D. Swern, in *Org. Peroxides*, Vol. 2 (Ed.: D. Swern), Interscience, New York, N. Y., **1971**, pp. 355-533.
- [8] B. Plesnicar, *Org. Chem. (N. Y.)* **1978**, *5*, 211-294.

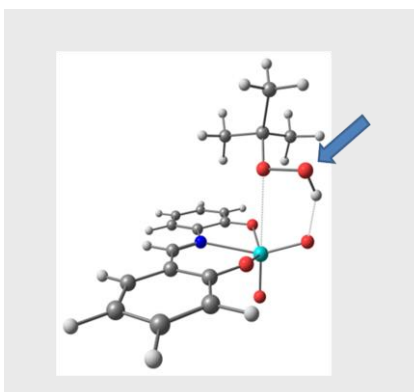
- [9] E. Rose, B. Andrioletti, S. Zrig, M. Quelquejeu-Etheve, *Chem. Soc. Rev.* **2005**, *34*, 573-583.
- [10] R. Mbeleck, K. Ambroziak, B. Saha, D. C. Sherrington, *React. Funct. Polym.* **2007**, *67*, 1448-1457.
- [11] S. K. Maiti, S. Dinda, R. Bhattacharyya, *Tetrahedron Lett.* **2008**, *49*, 6205-6208.
- [12] S. Kobayashi, K. Tahara, *Jpn. Kokai Tokkyo Koho* **2007**, JP 2007230908 A 2020070913.
- [13] M. Herbert, A. Galindo, F. Montilla, *Catal. Commun.* **2007**, *8*, 987-990.
- [14] K. A. Jørgensen, *Chem. Rev.* **1989**, *89*, 431-458.
- [15] R. A. Sheldon, I. Arends, U. Hanefeld, *Green Chemistry and Catalysis*, Wiley-VCH, Weinheim, **2007**.
- [16] M. Bagherzadeh, L. Tahsini, R. Latifi, L. K. Woo, *Inorg. Chim. Acta* **2009**, *362*, 3698-3702.
- [17] M. Yamazaki, H. Endo, M. Tomoyama, Y. Kurusu, *Bull. Chem. Soc. Japan* **1983**, *56*, 3523-3524.
- [18] J. C. Anderson, N. M. Smith, M. Robertson, M. S. Scott, *Tetrahedron Lett.* **2009**, *50*, 5344-5346.
- [19] K. Dallmann, R. Buffon, W. Loh, *J. Mol. Catal. A* **2002**, *178*, 43-46.
- [20] Regulation (EC) n° 1907/2006 of the European Parliament and Of the Council, *Official Journal of the European Union* **30.12.2006**, L396.
- [21] I. Sheikhsaie, A. Rezaeifard, N. Monadi, S. Kaafi, *Polyhedron* **2009**, *28*, 733-738.
- [22] R. Landau, G. A. Sullivan, D. Brown, *Chemtech* **1979**, *9*, 602-607.
- [23] P. Anastas, J. Warner, *Green Chemistry: Theory and Practice*, Oxford University Press, New York, **1998**.
- [24] P. Tundo, P. Anastas, D. S. Black, J. Breen, T. Collins, S. Memoli, J. Miyamoto, M. Polyakoff, W. Tumas, *Pure Appl. Chem.* **2000**, *72*, 1207-1228.
- [25] J. Kollar, *US 3,350,422 (1967); 3,351,635 (1967); 3,507,809 (1970); 3,625,981 (1971) to Halcon International.*
- [26] M. N. Sheng, G. J. Zajaczek, *GB 1.136.923 1968*.
- [27] M. J. Barber, P. J. Neame, *J. Biol. Chem.* **1990**, *265*, 20912-20915.
- [28] A. G. Wedd, *Coord. Chem. Rev.* **1996**, *154*, 5-11.
- [29] F. E. Kühn, A. M. Santos, A. D. Lopes, I. S. Goncalves, E. Herdtweck, C. C. Romao, *J. Mol. Catal. A* **2000**, *164*, 25-38.
- [30] A. Al-Ajlouni, A. A. Valente, C. D. Nunes, M. Pillinger, A. M. Santos, J. Zhao, C. C. Romão, I. S. Gonçalves, F. E. Kühn, *Eur. J. Inorg. Chem.* **2005**, 1716-1723.
- [31] S. M. Bruno, B. Monteiro, M. S. Balula, F. M. Pedro, M. Abrantes, A. A. Valente, M. Pillinger, P. Ribeiro-Claro, F. E. Kühn, I. S. Goncalves, *J. Mol. Catal. A* **2006**, *260*, 11-18.
- [32] X. G. Zhou, J. Zhao, A. M. Santos, F. E. Kühn, *Z. Naturforsch. B* **2004**, *59*, 1223-1228.
- [33] R. Martos Calvente, J. M. Campos-Martin, J. L. G. Fierro, *Catal. Commun.* **2002**, *3*, 247-251.
- [34] K. Ambroziak, B. Saha, R. Mbeleck, D. C. Sherrington, *J. Ion Exch.* **2007**, *18*, 598-603.
- [35] Y. Wang, Z. Q. Wu, Z. K. Li, X. G. Zhou, *Tetrahedron Lett.* **2009**, *50*, 2509-2511.
- [36] M. R. Pedrosa, J. Escribano, R. Aguado, V. Diez, R. Sanz, F. J. Arnaiz, *Polyhedron* **2007**, *26*, 3695-3702.
- [37] M. R. Pedrosa, R. Aguado, V. Diez, J. Escribano, R. Sanz, F. J. Arnaiz, *Eur. J. Inorg. Chem.* **2007**, 3952-3954.
- [38] D. Agustin, J.-C. Daran, R. Poli, *Acta Cryst. C* **2008**, *C64*, m101-m104.
- [39] D. Agustin, C. Bibal, B. Neveux, J.-C. Daran, R. Poli, *Z. Anorg. Allg. Chem.* **2009**, *635*, 2120-2125.
- [40] C. Zhang, G. Rheinwald, V. Lozan, B. Wu, P. G. Lassahn, H. Lang, C. Janiak, *Z. Anorg. Allg. Chem.* **2002**, *628*, 1259-1268.
- [41] Y. Sui, X. R. Zeng, X. N. Fang, X. K. Fu, Y. A. Xiao, L. Chen, M. H. Li, S. Cheng, *J. Mol. Catal. A* **2007**, *270*, 61-67.
- [42] A. N. Papadopoulos, C. P. Raptopoulos, A. Terzis, A. G. Hatzidimitriou, A. Gourdon, D. P. Kessissoglou, *J. Chem. Soc., Dalton Trans.* **1995**, 2591-2598.
- [43] M. Cindric, G. Galin, D. Matkovi-Calogovic, P. Novak, T. Hrenar, I. Ljubic, T. K. Novak, *Polyhedron* **2009**, *28*, 562-568.
- [44] J. Topich, J. T. Lyon, *Inorg. Chem.* **1984**, *23*, 3202-3206.
- [45] J. Topich, J. T. Lyon, *Polyhedron* **1984**, *3*, 55-60.
- [46] S. Colonna, A. Manfredi, M. Spadoni, L. Casella, M. Gullotti, *J. Chem. Soc., Perkin Trans. 1* **1987**, 71-73.
- [47] R. H. Holm, *Chem. Rev.* **1987**, *87*, 1401-1449.
- [48] W. S. Jung, H. Y. Moon, Y. Y. Park, *Polyhedron* **1997**, *16*, 2169-2173.
- [49] J. Liimatainen, A. Lehtonen, R. Sillanpaa, *Polyhedron* **2000**, *19*, 1133-1138.
- [50] M. Cindric, N. Strukan, V. Vrdoljak, B. Kamenar, *Z. Anorg. Allg. Chem.* **2004**, *630*, 585-590.
- [51] J. Zhao, X. G. Zhou, A. M. Santos, E. Herdtweck, C. C. Romao, F. E. Kühn, *Dalton Trans.* **2003**, 3736-3742.
- [52] J. M. Sobczak, J. J. Ziolkowski, *Appl. Catal. A* **2003**, *248*, 261-268.
- [53] A. Rezaeifard, I. Sheikhsaie, N. Monadi, M. Alipour, *Polyhedron* **2010**, *29*, 2703-2709.
- [54] A. Rezaeifard, I. Sheikhsaie, N. Monadi, H. Stoeckli-Evans, *Eur. J. Inorg. Chem.* **2010**, 799-806.
- [55] X. L. Wang, G. D. Wu, J. P. Li, N. Zhao, W. Wei, Y. H. Sun, *J. Mol. Catal. A* **2007**, *276*, 86-94.
- [56] Y. D. Li, X. K. Fu, B. W. Gong, X. C. Zou, X. B. Tu, J. X. Chen, *J. Mol. Catal. A* **2010**, *322*, 55-62.
- [57] footnote1.
- [58] footnote2.
- [59] O. A. Rajan, A. Chakravorty, *Inorg. Chem.* **1981**, *20*, 660-664.
- [60] T. Glowiak, L. Jerzykiewicz, J. A. Sobczak, J. J. Ziolkowski, *Inorg. Chim. Acta* **2003**, *356*, 387-392.
- [61] J. U. Mondal, F. A. Schultz, T. D. Brennan, W. R. Scheidt, *Inorg. Chem.* **1988**, *27*, 3950-3956.
- [62] J. M. Sobczak, T. Glowiak, J. J. Ziolkowski, *Trans. Met. Chem.* **1990**, *15*, 208-211.
- [63] M. Cindric, N. Strukan, V. Vrdoljak, T. Kajfez, B. Kamenar, *Z. Anorg. Allg. Chem.* **2002**, *628*, 2113-2117.
- [64] C. Cordelle, D. Agustin, J.-C. Daran, R. Poli, *Inorg. Chim. Acta* **2010**, *364*, 144-149.
- [65] J. Pisk, D. Agustin, V. Vrdoljak, R. Poli, *Adv. Synth. Catal.* **2011**, *353*, 2910-2914.
- [66] J. Pisk, B. Prugovečki, D. Matković-Čalogović, R. Poli, D. Agustin, V. Vrdoljak, *Polyhedron* **2012**, *33*, 441-449.
- [67] W. R. Thiel, *J. Mol. Catal. A* **1997**, *117*, 449-454.
- [68] D. D. Agarwal, S. Shrivastava, *Polyhedron* **1988**, *7*, 2569-2573.
- [69] Z. Dawoodi, R. L. Kelly, *Polyhedron* **1986**, *5*, 271-275.
- [70] W. R. Thiel, T. Priemeier, *Angew. Chem. Engl.* **1995**, *34*, 1737-1738.
- [71] W. R. Thiel, J. Eppinger, *Chem. Eur. J.* **1997**, *3*, 696-705.
- [72] L. F. Veiros, A. Prazeres, P. J. Costa, C. C. Romão, F. E. Kühn, M. J. Calhorda, *Dalton Trans.* **2006**, 1383-1389.
- [73] P. J. Costa, M. J. Calhorda, F. E. Kühn, *Organometallics* **2010**, *29*, 303-311.
- [74] A. Comas-Vives, A. Lledós, R. Poli, *Chem. Eur. J.* **2010**, *16*, 2147-2158.
- [75] C. Dinoi, M. Ciclosi, E. Manoury, L. Maron, L. Perrin, R. Poli, *Chem. Eur. J.* **2010**, *16*, 9572-9584.
- [76] A. M. Al-Ajlouni, D. Veljanovski, A. Capapé, J. Zhao, E. Herdtweck, M. J. Calhorda, F. E. Kühn, *Organometallics* **2009**, *28*, 639-645.
- [77] D. V. Deubel, J. Sundermeyer, G. Frenking, *Org. Lett.* **2001**, *3*, 329-332.
- [78] P. Gisdakis, I. V. Yudanov, N. Rösch, *Inorg. Chem.* **2001**, *40*, 3755-3765.
- [79] K. B. Sharpless, J. M. Townsend, D. R. Williams, *J. Am. Chem. Soc.* **1972**, *94*, 295-296.
- [80] H. Mimoun, I. Sere de Roch, L. Sajus, *Tetrahedron* **1970**, *26*, 37-50.
- [81] K. Uzarevic, M. Rubcic, I. Dilovic, Z. Kokan, D. Matkovic-Calogovic, M. Cindric, *Crystal Growth & Design* **2009**, *9*, 5327-5333.
- [82] J.-E. Jee, A. Comas-Vives, C. Dinoi, G. Ujaque, R. van Eldik, A. Lledós, R. Poli, *Inorg. Chem.* **2007**, *46*, 4103-4113.
- [83] R. Poli, *Comm. Inorg. Chem.* **2009**, *30*, 177-228.
- [84] P. D. Bartlett, *Record Chem. Progress* **1950**, *11*, 47-51.
- [85] R. D. Bach, C. Canepa, J. E. Winter, P. E. Blanchette, *J. Org. Chem.* **1997**, *62*, 5191-5197.
- [86] R. D. Bach, M. N. Glukhovtsev, C. Gonzalez, M. Marquez, C. M. Estevez, A. G. Baboul, H. B. Schlegel, *J. Phys. Chem. A* **1997**, *101*, 6092-6100.
- [87] K. N. Houk, J. Liu, N. C. DeMello, K. R. Condroski, *J. Am. Chem. Soc.* **1997**, *119*, 10147-10152.
- [88] G. J. J. Chen, J. W. McDonald, W. E. Newton, *Inorg. Chem.* **1976**, *15*, 2612-2615.
- [89] M. J. Frisch, G. W. Trucks, H. B. Schlegel, G. E. Scuseria, M. A. Robb, J. C. Cheeseman, J. Montgomery, J. A., T. Vreven, K. N. Kudin, J. C. Burant, J. M. Millam, S. S. Iyengar, J. Tomasi, V. Barone, B. Mennucci, M. Cossi, G. Scalmani, N. Rega, G. A. Petersson, H. Nakatsuji, M. Hada, M. Ehara, K. Toyota, R. Fukuda, J. Hasegawa, M. Ishida, T. Nakajima, Y. Honda, O. Kitao, H. Nakai, M. Klene, X. Li, J. E. Knox, H. P. Hratchian, J. B. Cross, C. Adamo, J. Jaramillo, R. Gomperts, R. E. Stratmann, O.

- Yazyev, A. J. Austin, R. Cammi, C. Pomelli, J. W. Ochterski, P. Y. Ayala, K. Morokuma, G. A. Voth, P. Salvador, J. J. Dannenberg, V. G. Zakrzewski, S. Dapprich, A. D. Daniels, M. C. Strain, O. Farkas, D. K. Malick, A. D. Rabuck, K. Raghavachari, J. B. Foresman, J. V. Ortiz, Q. Cui, A. G. Baboul, S. Clifford, J. Cioslowski, B. B. Stefanov, G. Liu, A. Liashenko, P. Piskorz, I. Komaromi, R. L. Martin, D. J. Fox, T. Keith, M. A. Al-Laham, C. Y. Peng, A. Nanayakkara, M. Challacombe, P. M. W. Gill, B. Johnson, W. Chen, M. W. Wong, C. Gonzalez, J. A. Pople, *Gaussian 03, Revision D.01*, Gaussian, Inc., Wallingford CT, **2004**.
- [90] A. D. Becke, *J. Chem. Phys.* **1993**, *98*, 5648-5652.
- [91] C. T. Lee, W. T. Yang, R. G. Parr, *Phys. Rev. B* **1988**, *37*, 785-789.
- [92] B. Miehlich, A. Savin, H. Stoll, H. Preuss, *Chem. Phys. Lett.* **1989**, *157*, 200-206.
- [93] R. Ditchfield, W. J. Hehre, J. A. Pople, *J. Chem. Phys.* **1971**, *54*, 724-728.
- [94] W. Hehre, R. Ditchfie, J. Pople, *J. Chem. Phys.* **1972**, *56*, 2257-2261.
- [95] P. C. Hariharan, J. A. Pople, *Theor. Chim. Acta* **1973**, *28*, 213-222.
- [96] P. C. Hariharan, J. A. Pople, *Mol. Phys.* **1974**, *27*, 209-214.
- [97] W. J. Stevens, H. Basch, M. Krauss, *J. Chem. Phys.* **1984**, *81*, 6026-6033.
- [98] W. J. Stevens, M. Krauss, H. Basch, P. G. Jasien, *Canad. J. Chem.* **1992**, *70*, 612-630.
- [99] T. R. Cundari, W. J. Stevens, *J. Chem. Phys.* **1993**, *98*, 5555-5565.
- 
- Received: ((will be filled in by the editorial staff))  
Published online: ((will be filled in by the editorial staff))
-

## Entry for the Table of Contents (Please choose one layout)

### FULL PAPER

[MoO<sub>2</sub>L]<sub>2</sub> complexes (L=SAP, SAE, SAMP) are active and selective pre-catalysts for the epoxidation of cyclooctene using TBHP in water as oxidant and no extra solvent. According to the DFT study; the TBHP oxidant coordinates 5-coordinated [MoO<sub>2</sub>(SAP)] as a neutral molecule; the way in which this transfers the O atom to the external olefin is reminiscent of Bartlett's epoxidation by peroxyacids.



*Julien Morlot, Nicolas Uyttebroeck, Dominique Agustin\*, Rinaldo Poli\**

**Page No. – Page No**

**Solvent-free epoxidation of olefins catalyzed by “[MoO<sub>2</sub>(SAP)]”: a new mode of TBHP activation**